Research on Chemical Intermediates
https://doi.org/10.1007/s11164-018-3691-7

Synthesis and photophysical properties of europium pentafluorinated β-diketonate complexes

Yupeng Wan[1] · **Heng Lyu**[1] · **Hengyi Du**[1] · **Dunjia Wang**[1] · **Guodong Yin**[1]

Received: 5 September 2018 / Accepted: 28 November 2018

Abstract

Two pentafluorinated β-diketone ligands, 4,4,5,5,5-pentafluoro-1-(4-methoxyphenyl)pentane-1,3-dione (PFMP) and 4,4,5,5,5-pentafluoro-1-(4-dimethyl aminophenyl)pentane-1,3-dione (PFAP), had been employed to synthesize six novel europium (III) complexes with ancillary ligands 2,2-dipyridine, 1,10-phenanthroline and 4,7-diphenyl-1,10-phenanthroline. The synthesized europium (III) complexes were characterized by FTIR, ^{1}H NMR, UV–Vis, luminescence spectroscopy, elemental analysis and thermogravimetric analysis. The photoluminescence spectra of these complexes showed the typical europium (III) red emissions in solid state and chloroform solution, assigned to $^5D_0 \rightarrow {}^7F_j$ ($j=0$–4) transitions. The higher values of intensity parameter Ω_2 indicated that the europium ion was in a highly polarizable ligand field in these complexes. Europium (III) complexes with the β-diketone PFMP exhibited much better photoluminescence properties than complexes with the β-diketone PFAP. Especially, the europium (III) complex of the β-diketone PFMP with the auxiliary ligand 2,2-dipyridine displayed the longest lifetime value, the highest quantum yield and good CIE color coordinates matching the pure red color ($x=0.67$, $y=0.33$) in these complexes. In addition, the proposed energy transfer mechanisms and the thermal stability of these complexes were also investigated and analyzed.

Keywords Europium complex · Pentafluorinated β-diketone · Photoluminescence · Quantum efficiency · Luminescent lifetime · Thermal analysis

---

Electronic supplementary material The online version of this article (https://doi.org/10.1007/s11164-018-3691-7) contains supplementary material, which is available to authorized users.

✉ Dunjia Wang
dunjiawang@163.com

[1] College of Chemistry and Chemical Engineering, Hubei Key Laboratory of Pollutant Analysis and Reuse Technology, Hubei Normal University, Huangshi 435002, China

Introduction

Europium complexes with various organic ligands have attracted more and more attention in materials [1], chemistry [2], biology [3], and physics [4] due to their advantageous spectroscopic characteristics such as extremely sharp emission spectrum, millisecond lifetime, large Stokes shifts and high quantum efficiency [5–7]. Luminescent europium complexes have many useful applications in optoelectronic devices [8], luminescent probes [9], bioassays [10], optical communications and tunable lasers [11]. In these complexes, europium β-diketonate complexes are an ideal series of molecules to study the influences of various parameters on luminescence and the quantum efficiency. In addition, the type of β-diketone and auxiliary ligand can be varied readily leading to controlled changes in the electronic effects as well as in the steric effects. Therefore, many researchers have reported the preparation and photoluminescence properties of some new europium β-diketonate complexes in the past decades [12–15]. Meanwhile, some europium fluorinated β-diketonate complexes were presented and exhibited the highly luminescent behaviors, which were due to the lower vibrational energy of the fluorinated ligands and the better volatility, thermal and oxidative stability of europium complexes [16–20].

Recently, we also reported some new europium β-diketonate complexes and investigated their spectroscopic and luminescent behaviors [21–23]. However, there have been very limited reports on europium pentafluorinated β-diketonate complexes up to now [24–27]. To further study the relationship between the β-diketone ligands and the photoluminescence properties of europium complexes, two fluorinated β-diketones with aromatic and pentafluoro-aliphatic substituents were synthesized and the photophysical properties of their europium complexes were investigated in detail. In this work, the polyfluorinated β-diketone ligands, 4,4,5,5,5-pentafluoro-1-(4-methoxyphenyl)pentane-1,3-dione (PFMP) and 4,4,5,5,5-pentafluoro-1-(4-dimethylaminophenyl)pentane-1,3-dione (PFAP), were synthesized by the Claisen condensation. With these two pentafluorinated β-diketones as the first ligand and 2,2-dipyridine (Bipy), 1,10-phenanthroline (Phen) or 4,7-diphenyl-1,10-phenanthroline (Bath) as the auxiliary ligand, six new europium β-diketonate complexes, $\mathrm{Eu(PFMP)_3 \cdot Bipy}$, $\mathrm{Eu(PFAP)_3 \cdot Bipy}$, $\mathrm{Eu(PFMP)_3 \cdot Phen}$, $\mathrm{Eu(PFAP)_3 \cdot Phen}$, $\mathrm{Eu(PFMP)_3 \cdot Bath}$ and $\mathrm{Eu(PFAP)_3 \cdot Bath}$, were synthesized and characterized. Their photophysical and thermal behaviors were investigated as well. Additionally, the experimental intensity parameters (Ω_2 and Ω_4), nonradiative (A_{nrad}), radiative (A_{rad}), luminescence lifetime (τ) and intrinsic quantum yield (Φ_{Ln}) were calculated and analyzed. The results prompted us to further explain the photoluminescence properties of these europium complexes.

Experimental

Materials and measurements

Europium (III) chloride hexahydrate, ethyl pentafluoropropionate and sodium were obtained from J&K Chemical (Shanghai) Ltd. The 4-Dimethylaminoacetophenone, 4-methoxyacetophenone, 1,10-phenanthroline, 4,7-Diphenyl-1,10-phenanthroline and 2,2-dipyridine were purchased from Sun Chemical Technology (Shanghai) Ltd. Other reagents used were of analytical grade or were purified using standard procedures.

Elemental analysis was performed on an elemental analyzer (Perkin-Elmer, 2400CHN). Europium contents were determined by EDTA complexometry. Melting points were determined on an X-4 digital micro-melting-point apparatus. ^{1}H NMR spectra were recorded on an NMR spectrometer (Bruker, Avance III^{TM} 300 MHz) in $CDCl_3$ media. IR spectra were obtained on an infrared spectrophotometer (Nicolet, FTIR 5700) in KBr pellets. ESI–MS measurements were measured on a mass spectrometer (Finnigan, LCQ Advantage Max). Absorption spectra were recorded with a UV–Vis spectrophotometer (Hitachi, U-3010). Photoluminescence spectra and lifetime values were measured at room temperature with a fluorescence spectrometer (Varian, Cary Eclipse). Photoluminescence quantum yields (Φ) were measured with quinine sulfate in 0.1 mol L^{-1} sulfuric acid ($\Phi_s = 0.55$, $\lambda_{ex} = 366$ nm) as a standard at room temperature [28, 29]. Thermogravimetric analysis was carried on a simultaneous thermal analyzer (Netzsch STA 449F5) from 50 to 1100 °C at a heating rate of 10 °C/min under nitrogen atmosphere.

Synthesis of pentafluorinated β-diketones

4,4,5,5,5-Pentafluoro-1-(4-methoxyphenyl)pentane-1,3-dione (PFMP): The freshly cut sodium (0.69 g, 30 mmol) and ethanol (30 mL) were added into a 100 mL round bottom flask with magnetic stirring and were heated till sodium was exhausted. The excess ethanol was removed by rotary evaporation, and the residue was dissolved in tetrahydrofuran (30 mL). To this suspension solution, 4-methoxyacetophenone (2.0 g, 13 mmol) and ethyl pentafluoropropionate (20 mL) were added and stirred for 8 h at room temperature. The organic solvent was evaporated and the deionized water (50 mL) was added into the resulting mixture. Then, the mixture was adjusted to pH = 6 with dilute hydrochloric acid and the yellow solid was precipitated. The solid was recrystallized with 1:2 (v/v) chloroform-petroleum ether to give the light yellow crystal PFMP in yield 70%. Mp 153–154 °C; IR (KBr): ν 3436 (b, m), 3027 (m), 2925(m), 2849 (w), 1632 (s), 1601 (s), 1506 (s), 1400 (m), 1325 (m), 1251 (s), 1212 (m), 1172 (s), 1067 (m), 1029 (m), 846 (m), 810 (s), 705 (m), cm^{-1}; ^{1}H NMR (300 MHz, $CDCl_3$): δ 3.90 (s, 3H, OCH_3), 6.57 (s, 1H, enol CH), 6.99 (d, 2H, Ar–H, $J = 8.7$ Hz), 7.95 (d, 2H, Ar–H, $J = 8.7$ Hz), 15.62 (brs, 1H, enol OH) ppm; ESI–MS: m/z 297.03 $[M+H]^+$. Anal. Calcd. for $C_{12}H_9O_3F_5$: C, 48.66; H, 3.06; Found C, 48.89; H, 3.01.

4,4,5,5,5-Pentafluoro-1-(4-dimethylaminophenyl)pentane-1,3-dione (PFAP): The synthetic method of β-diketone PFAP was the same as that of the compound PFMP and the yellow crystal PFAP was obtained in a yield of 75%. Mp 209–210 °C; IR (KBr): ν 3441 (b, m), 3036 (m), 2927 (m), 2853 (m), 1631 (s), 1600 (s), 1512 (s), 1398 (m), 1270 (m), 1187 (s), 1067 (m), 1007 (m), 1063 (s), 1013 (m), 791 (s), 696 (m) cm^{-1}; ^1H NMR (300 MHz, $CDCl_3$): δ 3.11 (s, 6H, $N(CH_3)_2$), 6.49 (s, 1H, enol CH), 6.68 (d, 2H, Ar–H, $J=8.7$ Hz), 7.86 (d, 2H, Ar–H, $J=8.7$ Hz), 16.00 (brs, 1H, enol OH) ppm; ESI–MS: m/z 310.08 $[M+H]^+$; Anal. Calcd. for $C_{13}H_{12}NO_2F_5$: C, 50.49; H, 3.91; N, 4.53; Found C, 50.76; H, 3.88; N, 4.49.

Synthesis of europium (III) complexes (C1–C6)

The synthetic procedure of europium (III) pentafluorinated β-diketonate complexes is below described: The pentafluorinated β-diketone ligand (3 mmol), NaOH (0.12 g, 3 mmol) and the auxiliary ligand (1 mmol) were dissolved in 30 mL ethanol and heated to 60 °C under stirring. Then, the ethanolic solution of $EuCl_3 \cdot 6H_2O$ (1 mmol) was added dropwise, and the reaction mixture was stirred at 60 °C for 8 h. After cooling down, the yellow solid was precipitated and filtered off. The solid product was washed with deionized water and ethanol, and dried in vacuum. The europium (III) complexes (**C1**–**C6**) were obtained.

$Eu(PFMP)_3 \cdot$Bipy (**C1**): Yellow powder, yield 80%, mp 191–193 °C; IR ν (KBr): 3032 (w), 2931 (m), 2843 (w), 1598 (s), 1569 (s), 1501 (s), 1327 (m), 1260 (s), 1171 (s), 1079 (m), 1011 (s), 930 (m), 845 (m), 788 (s), 588 (m), 506 (m) cm^{-1}; ^1H NMR (300 MHz, $CDCl_3$): δ 3.36 (s, 3H, C=CH), 3.96 (s, 9H, OCH_3), 6.91 (br, 6H, Ar–H), 7.71 (br, 6H, Ar–H), 8.77 (br, 2H, Bipy-H), 9.74 (br, 2H, Bipy-H), 10.34 (br, 2H, Bipy-H), 14.85 (br, 2H, Bipy-H) ppm. Anal. Calcd. for $EuC_{46}H_{32}N_2O_9F_{15}$: C, 46.28; H, 2.70; N, 2.35; Eu, 12.73; Found C, 46.57; H, 2.72; N, 2.31; Eu, 12.85.

$Eu(PFAP)_3 \cdot$Bipy (**C2**): Yellow powder, yield 85%, mp 189–191 °C; IR ν (KBr): 3021(m), 2921 (m), 2857 (m), 1586 (s), 1549 (s), 1506 (s), 1373 (m), 1281 (s), 1187 (s), 1079 (m), 1009 (m), 926 (m), 829 (m), 783 (s), 587 (m), 508 (m) cm^{-1}; ^1H NMR (300 MHz, $CDCl_3$): δ 3.09 (s, 3H, C=CH), δ 3.25 (s, 18H, $N(CH_3)_2$), 6.62 (br, 6H, Ar–H), 7.69 (br, 6H, Ar–H), 8.79 (br, 2H, Bipy-H), 9.82 (br, 2H, Bipy-H), 10.73 (br, 2H, Bipy-H), 14.18 (br, 2H, Bipy-H) ppm. Anal. Calcd. for $EuC_{49}H_{41}N_5O_6F_{15}$: C, 47.74; H, 3.35; N, 5.68; Eu, 12.33; Found C, 47.52; H, 3.31; N, 5.75; Eu, 12.18.

$Eu(PFMP)_3 \cdot$Phen (**C3**): Yellow powder, yield 82%, mp 211–213 °C; IR ν (KBr): 3026 (m), 2944 (m), 2842 (w), 1599 (s), 1571 (s), 1500 (s), 1328 (m), 1258 (s), 1174 (s), 1078 (m), 1009 (m), 928 (m), 843 (m), 788 (s), 592 (m), 509 (m) cm^{-1}; ^1H NMR (300 MHz, $CDCl_3$): δ 3.29 (s, 3H, C=CH), 3.95 (s, 9H, OCH_3), 6.87 (d, 6H, Ar–H, $J=8.0$ Hz), 7.61 (d, 6H, Ar–H, $J=8.1$ Hz), 8.72 (d, 2H, Phen-H, $J=7.7$ Hz), 9.78 (s, 2H, Phen-H), 10.41 (d, 2H, Phen-H, $J=7.9$ Hz), 11.25 (br, 2H, Phen-H) ppm. Anal. Calcd. for $EuC_{48}H_{32}N_2O_9F_{15}$: C, 47.34; H, 2.65; N, 2.30; Eu, 14.48; Found C, 47.68; H, 2.61; N, 2.35; Eu, 14.27.

$Eu(PFAP)_3 \cdot$Phen (**C4**): Yellow powder, yield 75%, mp 213–215 °C; IR ν (KBr): 3030 (m), 2935 (m), 2857 (m), 1587 (s), 1549 (s), 1506 (s), 1373 (m), 1280 (s), 1180 (s), 1079 (s), 1008 (m), 927 (m), 864 (m), 787 (s), 578 (m), 508 (m) cm^{-1}; ^1H NMR

(300 MHz, $CDCl_3$): δ 3.03 (s, 3H, C=CH), δ 3.32 (s, 18H, $N(CH_3)_2$), 6.68 (br, 6H, Ar–H), 7.65 (br, 6H, Ar–H), 8.80 (br, 2H, Phen-H), 10.01 (br, 2H, Phen-H), 10.52 (br, 2H, Phen-H), 11.11 (br, 2H, Phen-H) ppm. Anal. Calcd. for $EuC_{51}H_{41}N_5O_6F_{15}$: C, 48.74; H, 3.29; N, 5.57; Eu, 12.09; Found C, 49.08; H, 3.24; N, 5.65; Eu, 12.23.

$Eu(PFMP)_3$·Bath (**C5**): Yellow powder, yield 78%, mp 200–202 °C; IR ν (KBr): 3031(m), 2967 (m), 2843 (w), 1597 (s), 1572 (s), 1501 (s), 1258 (s), 1172 (s), 1082 (m), 1013 (m), 930 (m), 845 (m), 789 (s), 588 (m), 508 (m) cm^{-1}; ^1H NMR (300 MHz, $CDCl_3$): δ 3.70 (s, 3H, C=CH), 3.94 (s, 9H, OCH_3), 6.86 (br, 6H, Ar–H), 7.61 (br, 6H, Ar–H), 7.96 (br, 2H, Bath-H), 8.17 (br, 4H, Bath-H), 8.58 (br, 2H, Bath-H), 8.73 (br, 4H, Bath-H), 9.24 (br, 2H, Bath-H), 12.10 (br, 2H, Bath-H) ppm. Anal. Calcd. for $EuC_{60}H_{40}N_2O_9F_{15}$: C, 52.61; H, 2.94; N, 2.04; Eu, 11.09; Found C, 52.94; H, 2.91; N, 2.09; Eu, 11.25.

$Eu(PFAP)_3$·Bath (**C6**): Yellow powder, yield 75%, mp 180–182 °C; IR ν (KBr): 3027(m), 2922 (m), 2853 (m), 1592 (s), 1552 (s), 1506 (s), 1281 (s), 1187 (s), 1079 (m), 928 (m), 783 (s), 588 (m), 507 (m) cm^{-1}; ^1H NMR (300 MHz, $CDCl_3$): δ 2.98 (s, 3H, C=CH), δ 3.23 (s, 18H, $N(CH_3)_2$), 6.58 (br, 6H, Ar–H), 7.57 (br, 6H, Ar–H), 7.99 (br, 2H, Bath-H), 8.22 (br, 4H, Bath-H), 8.68 (br, 2H, Bath-H), 8.87 (br, 4H, Bath-H), 9.53 (br, 2H, Bath-H), 11.74 (br, 2H, Bath-H) ppm. Anal. Calcd. for $EuC_{63}H_{49}N_5O_6F_{15}$: C, 53.70; H, 3.51; N, 4.97; Eu, 10.79; Found C, 53.47; H, 3.47; N, 5.02; Eu, 10.93.

Results and discussion

Synthesis and characterization

The synthetic procedures for pentafluorinated β-diketones and their europium (III) complexes are shown in Scheme 1. The pentafluorinated β-diketones were synthesized from 4-methoxyacetophenone or 4-Dimethylaminoacetophenone by Claisen condensation with ethyl pentafluoropropionate in the presence of sodium ethoxide in tetrahydrofuran. The europium pentafluorinated β-diketonate complexes were synthesized from the pentafluorinated β-diketones and europium chloride hexahydrate with 2,2-dipyridine, 1,10-phenanthroline or 4,7-Diphenyl-1,10-phenanthroline in ethanol solution as described by the literature [30]. The complexes were characterized by elemental analysis, thermogravimetric analysis, ^1H NMR, FTIR and ESI–MS spectroscopy.

In ^1H NMR spectra of complexes **C1**–**C6**, there were well pronounced changes compared with those of the pentafluorinated β-diketones and auxiliary ligands, which was due to the paramagnetism of the europium ion. Firstly, the enolic proton chemical shifts at $\delta = 16.00–15.62$ ppm in pentafluorinated β-diketones disappeared completely in europium complexes. Secondly, the enolic methine proton shifts at $\delta = 6.57–6.49$ ppm in pentafluorinated β-diketones moved to high-field at $\delta = 3.70–2.98$ ppm in europium complexes, which was attributed to the closeness between these protons binding site and the paramagnetic europium ion [31, 32]. Thirdly, compared with the free auxiliary ligands, their aryl proton shifts displayed a very obvious downfield shift in europium complexes [33, 34]. In

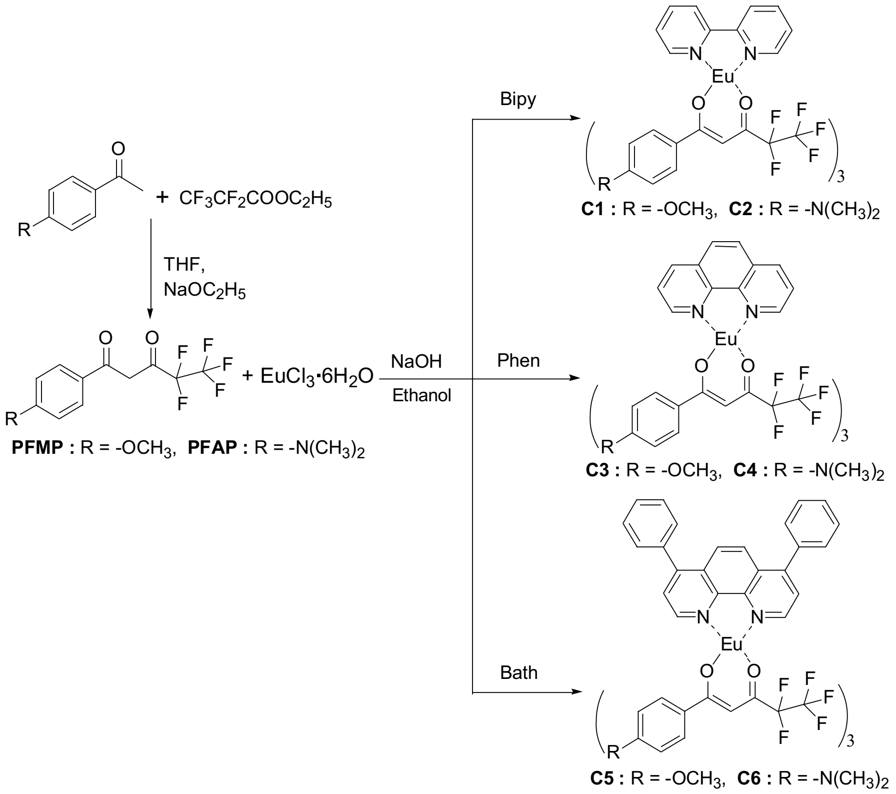

Scheme 1 Synthesis of pentafluorinated β-diketones and europium (III) complexes

addition, the aryl proton chemical shifts of pentafluorinated β-diketones moved a bit toward high-field in their europium complexes. Here, we took ^{1}H NMR spectrum of the complex **C3** (Fig. 1) as an example. From Fig. 1, the broad two-proton singlet at δ 11.25 ppm corresponded to H_a $H_{a'}$. The two two-proton doublets ($J = 7.9$ Hz, 7.7 Hz) at δ 10.41 and 8.72 ppm were attributed to H_c $H_{c'}$ and H_b $H_{b'}$, respectively. The singlet peak at δ 9.78 ppm was assigned to H_d $H_{d'}$. Protons H_f $H_{f'}$ and H_e $H_{e'}$ appeared as a six-proton doublet ($J = 8.1$ Hz, 8.0 Hz) at δ 7.61 and 6.87 ppm, respectively. Proton H_h exhibited a nine-proton singlet at δ 3.95 ppm and Proton H_g revealed a three-proton singlet at δ 3.29 ppm.

The characteristic FT-IR absorption bands of pentafluorinated β-diketones and their europium complexes are listed in Table 1. From Table 1, IR spectra of complexes **C1**–**C6** displayed the disappearance of the enolic O–H vibration bands (PFMP: 3436 cm^{-1}, PFAP: 3442 cm^{-1}) for the free β-diketone ligands. The strong vibration bands at 1632 cm^{-1}, 1601–1600 cm^{-1} and 1512–1506 cm^{-1} of β-diketone ligands were assigned to their keto form carbonyl C=O, enol form carbonyl C=O and enol form C=C stretching vibrations, respectively [35, 36]. But in complexes **C1**–**C6**, the strong keto form carbonyl C=O vibration

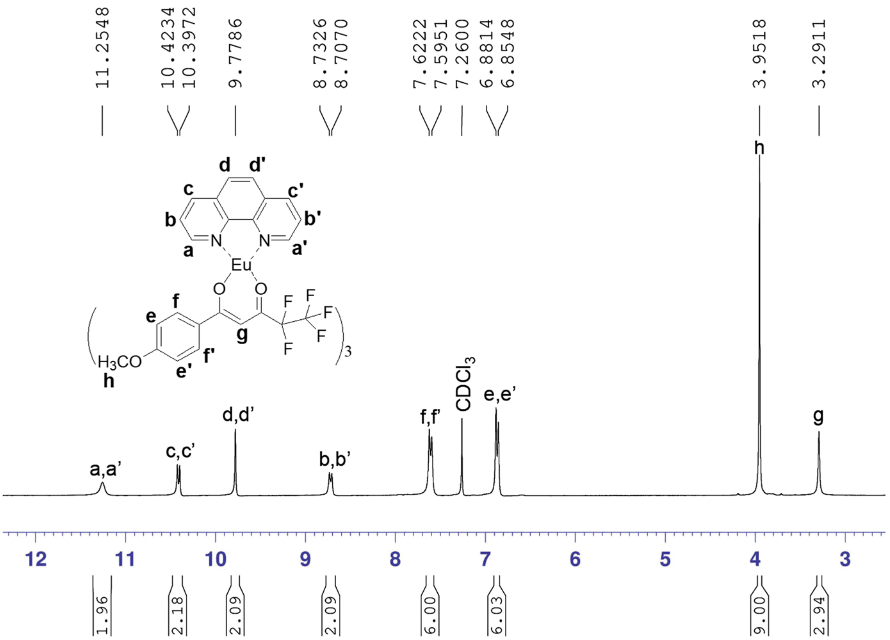

Fig. 1 ^{1}H NMR spectrum of the europium complex **C3** in $CDCl_3$

Table 1 Characteristic IR bands (cm^{-1}) of β-diketones and europium complexes

Compound	ν (O–H)	ν (C=O)	ν (C=N)	ν (C=C)	ν (Eu–N)	ν (Eu–O)
PFMP	3436 (m)	1632 (s) 1601 (s)	–	1506 (s)	–	–
PFAP	3442 (m)	1632 (s) 1600 (s)	–	1512 (s)	–	–
C1	–	1598 (s)	1569 (s)	1501 (s)	588 (m)	506 (m)
C2	–	1586 (s)	1549 (s)	1506 (s)	587 (m)	508 (m)
C3	–	1599 (s)	1571 (s)	1500 (s)	592 (m)	509 (m)
C4	–	1587 (s)	1549 (s)	1506 (s)	578 (m)	508 (m)
C5	–	1597 (s)	1572 (s)	1501 (s)	588 (m)	508 (m)
C6	–	1592 (s)	1552 (s)	1506 (s)	588 (m)	507 (m)

bands disappeared; the enolic C=O and C=C absorption bands down-shifted to 1599–1586 cm^{-1} and 1506–1501 cm^{-1}, respectively. These IR data indicated that the pentafluorinated β-diketone ligands were coordinated to the europium ions through the β-diketone enolic hydroxyl oxygen and carbonyl oxygen in complexes. Additionally, the strong absorption bands at 1549–1572 cm^{-1} in complexes were due to C=N stretching vibrations of the auxiliary ligands (Bipy, Phen or Bath). The new absorption bands observed at 592–578 cm^{-1} and 509–506 cm^{-1} in complexes exhibited the presence of the coordination bonds Eu–N and Eu–O, respectively [9, 37]. These results further confirmed the pentafluorinated β-diketone ligands and Bipy, Phen or Bath were coordinated to the europium ions through the enolic hydroxyl O, carbonyl O and heterocyclic N atoms.

Photophysical properties

UV–Vis absorption spectra

The UV–Vis electronic spectra of europium complexes **C1**–**C6** in chloroform solution (1×10^{-5} mol/L) are presented in Fig. 2, together with the free β-diketones and auxiliary ligands for comparison. From Fig. 2, the absorption bands of free pentafluorinated β-diketones were observed at 276–278 nm and 330–346 nm, which were assigned to the π–π* transitions in the phenyl rings and the characteristic π–π* enolic transitions of the free β-diketone ligands, respectively; those of auxiliary ligands were found at 276–278 nm, which were due to the π–π* transitions in the nitrogen donor heterocyclic ligands. Meanwhile, the absorption spectra of complexes **C1**–**C6** exhibited two strong absorption bands at 280–282 nm and 336–366 nm, which were red-shifted 2–6 nm compared with the corresponding absorption bands of nitrogen heterocyclic ligands and 6–20 nm in comparison with the corresponding enolic absorption bands of β-diketone ligands, respectively. These results indicated the formation of the large conjugated chelate systems between europium (III) ions and these ligands.

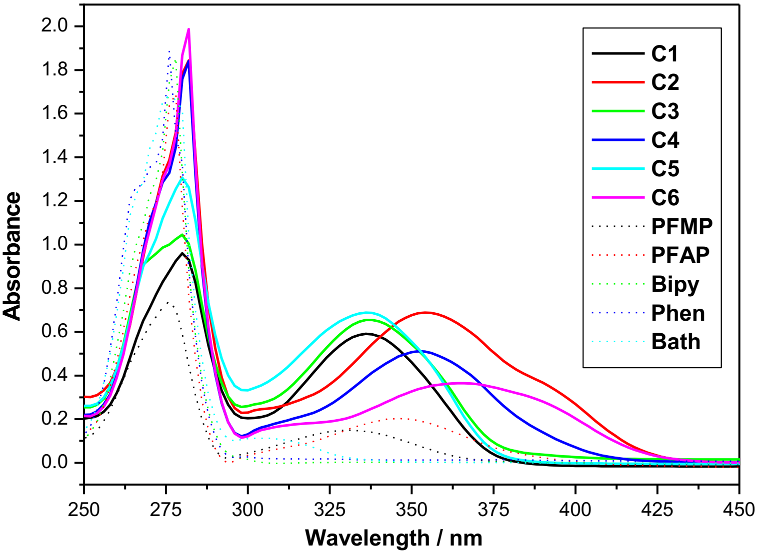

Fig. 2 UV–Vis spectra of ligands PFMP, PFAP, Bipy, Phen, Bath and europium complexes **C1**–**C6** in chloroform solution (1×10^{-5} mol/L)

Photoluminescence behavior

The photoluminescence behaviors of europium (III) pentafluorinated β-diketonate complexes in solid state were studied in detail at room temperature. The excitation spectra of europium (III) complexes **C1**–**C6** in solid powder were recorded by governing the hypersensitive $^5D_0 \rightarrow {}^7F_2$ emission band at 612 nm (Fig. 3). From Fig. 3, there was a much broader band between 250 and 400 nm in their excitation spectra; especially complex **C1** displayed a more intense and broad excitation band. The results strongly suggested an efficient sensitization process between organic ligands and the europium (III) ion. Meanwhile, a low-intensity and narrow lines at 465 nm associated with the europium (III) ion transition of $^7F_0 \rightarrow {}^5D_2$ were observed in their excitation spectra [38].

The emission spectra of europium (III) complexes **C1**–**C6** in solid state are depicted in Fig. 4 under excitation at 350 nm for complexes **C1**, **C3** and **C5** (380 nm for complexes **C2**, **C4** and **C6**). From Fig. 4, these complexes displayed the characteristic narrow emission bands at about 580, 592, 613, 652, and 704 nm, which were due to the $^5D_0 \rightarrow {}^7F_0$, $^5D_0 \rightarrow {}^7F_1$, $^5D_0 \rightarrow {}^7F_2$, $^5D_0 \rightarrow {}^7F_3$ and $^5D_0 \rightarrow {}^7F_4$ transitions of the europium (III) ion, respectively. The weak intensity emission bands at about 580 and 652 nm were attributed to the forbidden transitions in magnetic and electric dipoles for $^5D_0 \rightarrow {}^7F_0$ and $^5D_0 \rightarrow {}^7F_3$ transition. Meanwhile, the presence of the only one sharp emission peak corresponding to the $^5D_0 \rightarrow {}^7F_0$ transition indicated the existence of one local site of symmetry for europium (III) complexes [39]. The relatively strong emission band at about 592 nm was independent of the local chemical environment, which was due to the magnetic dipole transition $^5D_0 \rightarrow {}^7F_1$.

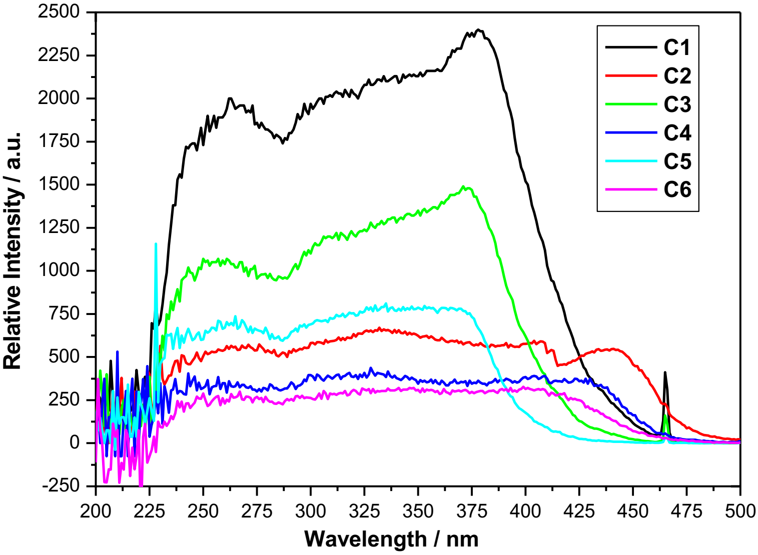

Fig. 3 Room-temperature excitation spectra of europium complexes **C1**–**C6** in solid state monitored at 612 nm

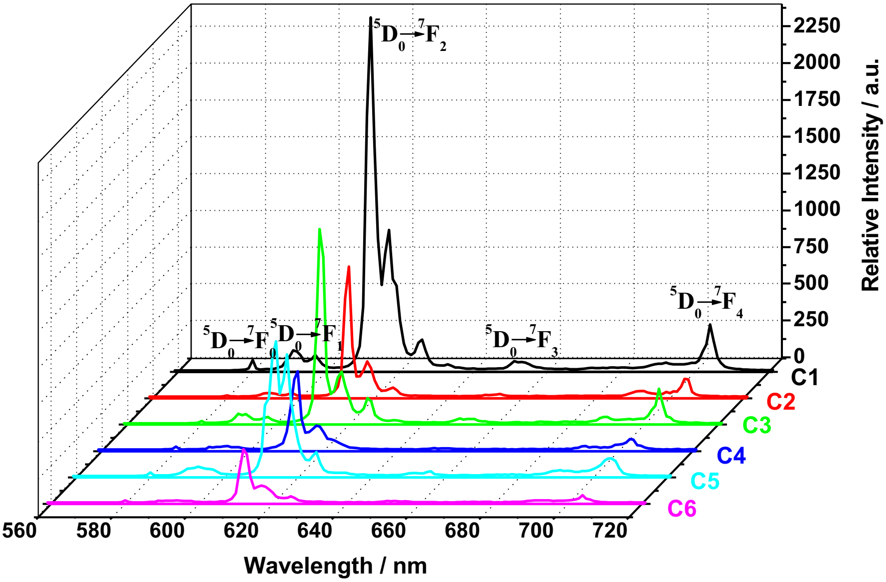

Fig. 4 Room-temperature emission spectra of europium complexes **C1**–**C6** in solid state under excitation at 350, 380, 350, 380, 350 and 380 nm, respectively

The strongest emission band at about 613 nm corresponding to $^5D_0 \rightarrow ^7F_2$ transition was an induced electric dipole transition and a highly polarizable coordination environment around the europium (III) ion, leading to the brilliant red emission of these europium (III) complexes [4]. It was evidently observed that europium (III) complexes (**C1**, **C3** and **C5**) with the first ligand PFMP exhibited much higher photoluminescence intensities in comparison with complexes (**C2**, **C4** and **C6**) with the ligand PFAP, which was probably due to the much stronger fluorescence quenching effect of *N*,*N*-dimethylamino moieties in europium (III) complexes.

The CIE color coordinates (x, y) of europium (III) complexes **C1**–**C6** were calculated from their emission spectra in solid state and presented in Fig. 5. The results displayed that their chromaticity coordinates were ($x=0.669$, $y=0.331$), ($x=0.615$, $y=0.385$), ($x=0.668$, $y=0.332$), ($x=0.550$, $y=0.449$), ($x=0.671$, $y=0.329$) and ($x=0.604$, $y=0.395$) for europium (III) complexes **C1**–**C6** respectively. Obviously, the CIE color coordinates of complexes **C1**, **C3** and **C5** were very close to the NTSC (1931) standard values for red ($x=0.67$, $y=0.33$) [40], and they would be a good candidate as a red component for the preparation of OLEDs.

The photoluminescence spectra of europium (III) complexes **C1**–**C6** in chloroform solution (1×10^{-5} mol/L) were also measured (Fig. 6). From Fig. 6, complexes **C1**–**C6** also exhibited the characteristic emissions at about 580, 593, 612, 651, and 701 nm for the europium (III) ion, and they were similar to these complexes in solid state. However, the emission peaks in solution were somewhat broadened and little or no splitting compared with those in solid state, presumably because of the intermolecular interactions between ligands and solvent resulting in the high frequency oscillation. Meanwhile, photoluminescence quantum yields (Φ) of these complexes

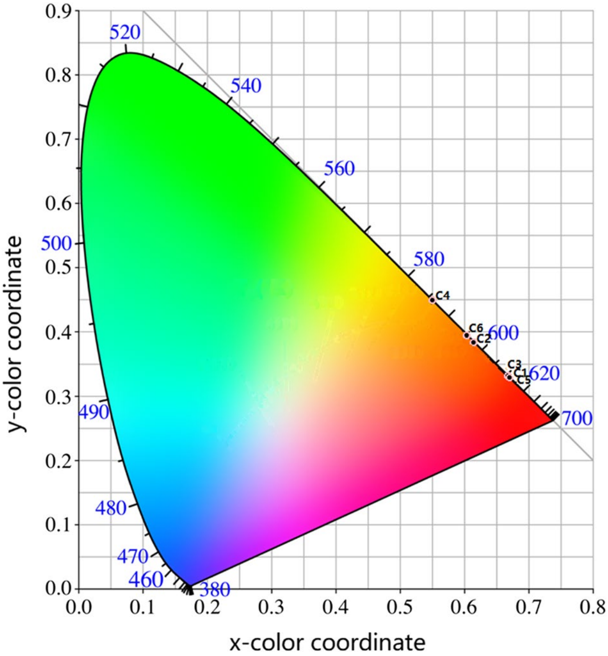

Fig. 5 The CIE chromaticity diagram of europium complexes **C1−C6** in solid state

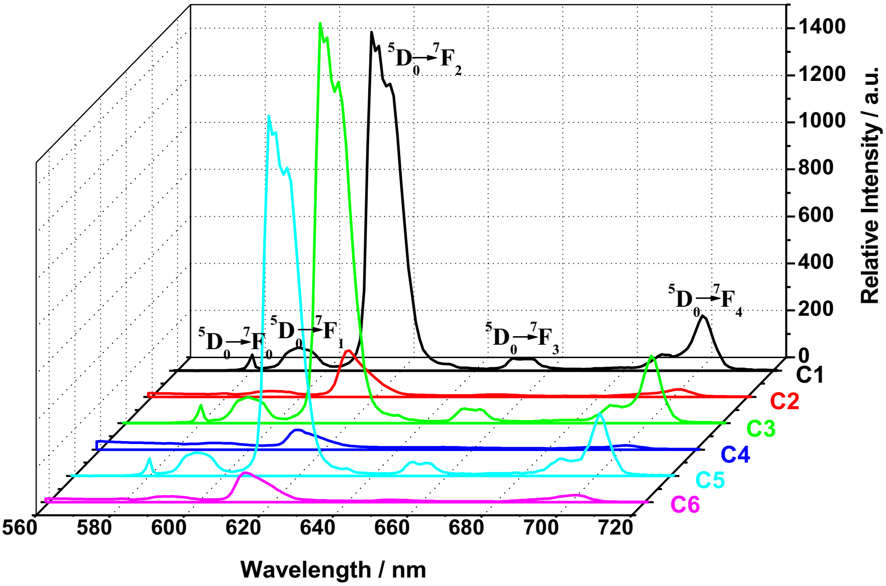

Fig. 6 Emission spectra of europium complexes **C1−C6** in chloroform solution (1×10^{-5} mol/L) under excitation at 350, 380, 350, 380, 350 and 380 nm, respectively

Table 2 Photoluminescence data of complexes **C1**–**C6** in solid state and solution

Complex	In solid state						In solution
	τ (μs)	A_{rad} (s^{-1})	A_{nrad} (s^{-1})	Ω_2 (10^{-20} cm^2)	Ω_4 (10^{-20} cm^2)	Φ_{Ln} (%)	Φ (%)
C1	814	773	414	18.74	3.01	62.9	37.5
C2	350	1060	1797	25.01	6.02	37.1	5.5
C3	741	812	538	18.89	4.35	60.1	37.1
C4	267	935	2810	22.30	4.89	25.0	5.9
C5	735	820	541	19.84	3.59	60.2	32.8
C6	233	1026	3266	25.15	4.26	23.9	5.5

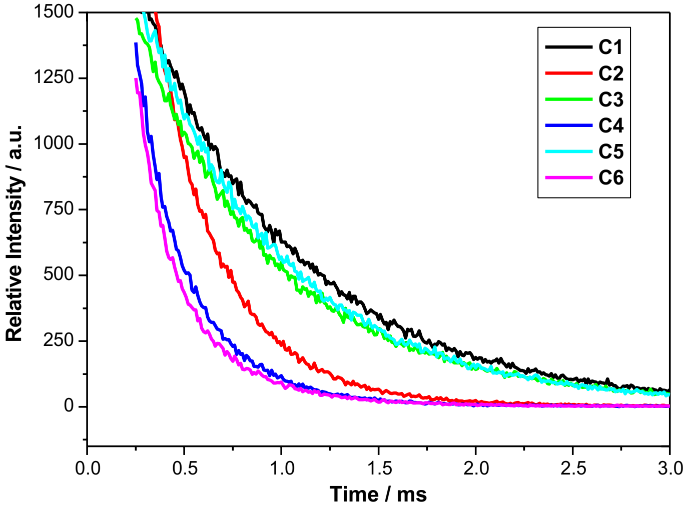

Fig. 7 Room-temperature luminescence decay curves of europium complexes **C1**–**C6** in solid state monitored at 612, 613, 612, 613, 614 and 612 nm, respectively

in chloroform were measured relative to quinine sulfate (Φs = 0.55) and the data were depicted in Table 2. It was clearly found that complexes (**C1**, **C3** and **C5**) based on PFMP as ligand exhibited much higher photoluminescence quantum yields (Φ = 37.5%, 37.1% and 32.8%, respectively) and much stronger photoluminescent intensities than complexes (**C2**, **C4** and **C6**) based on PFAP as ligand. These results were possibly due to the higher frequency oscillation for the ligand PFAP containing *N*,*N*-dimethylamino moiety in solutions to quench the europium (III) ion excited states nonradiatively [41].

The decay curve pattern of europium (III) complexes **C1**–**C6** were also determined by monitoring the emission lines ($^5D_0 \rightarrow {}^7F_2$) at about 612 nm in solid state. As shown in Fig. 7, these luminescence decay curves were well fitted into a single exponential function $I(t) = I_0 \exp(-t/\tau)$ where I_0 is the intensity at time 0 and τ is the decay time for radiative emission [42]. The results suggested the presence of a single chemical environment around the emitting europium (III) ion in complexes **C1**–**C6**, which was consistent with the results of the only one $^5D_0 \rightarrow {}^7F_0$ line in emission spectra. The luminescence lifetime values (τ) calculated from the decay curves of these europium (III) complexes are presented in Table 2. The relatively shorter lifetime values (τ) observed for europium complexes **C2**, **C4** and **C6** could result from dominant nonradiative decay channels associated with high-energy oscillators because of the presence of *N*,*N*-dimethylamino moieties, as well documented in some europium complexes [29]. Meanwhile, the longer lifetime values (τ) had been observed for complexes **C1**, **C3** and **C5** owing to the less nonradiative decay pathways.

The intrinsic luminescent quantum yield (Φ_{Ln}) for complexes **C1**–**C6** can be calculated by their emission spectra data and lifetime values (τ), which represented the ratio of radiative to nonradiative processes in the ligand field of europium (III) ion [24].

$$\Phi_{Ln} = \frac{A_{rad}}{A_{rad} + A_{nrad}} \tag{1}$$

The radiative (A_{rad}) rates can be obtained by summing the radiative rates of each $^5D_0 \rightarrow {}^7F_J$ transition ($\Sigma_J A_{0J}$) of the europium (III) ion and A_{0J} can be determined through the following equation [5].

$$A_{0J} = A_{01} \frac{I_{0J}}{I_{01}} \frac{\nu_{01}}{\nu_{0J}}, \tag{2}$$

where I_{0J} and ν_{0J} are the integrated intensities and energy barycenters of the $^5D_0 \rightarrow {}^7F_J$ transitions ($J = 1$, 2 and 4), respectively. A_{01} is the Einstein's coefficient of spontaneous emission between the $^5D_0$ and $^7F_1$ energy levels and its value can be estimated as 50 s^{-1} approximately in an air atmosphere [43].

The radiative (A_{rad}) and nonradiative (A_{nrad}) processes were involved in the depopulation of the emitting $^5D_0$ state and depended on the luminescence lifetime (τ) of the state $^5D_0$ as shown in the following equation [5]:

$$\frac{1}{\tau} = A_{rad} + A_{nrad}. \tag{3}$$

The estimated photoluminescence data of europium complexes **C1**–**C6** (A_{rad}, A_{nrad} and Φ_{Ln}) are reported in Table 2. From Table 2, the calculated intrinsic quantum yields (Φ_{Ln}) of these complexes were in accord with the measured photoluminescence quantum yields (Φ) in chloroform solution. The nonradiative transition rates (A_{nrad}) of europium complexes **C2**, **C4** and **C6** were clearly much larger than those of complexes **C1**, **C3** and **C5**. It indicated that the introduction of *N*,*N*-dimethylamino moieties in complexes **C2**, **C4** and **C6** increased the quenching phenomena resulting from a large number of high-frequency oscillators C-H bonds as well as the radiative energy losses. As a consequence, europium complexes **C2**, **C4** and **C6** based on the pentafluorinated β-diketone PFAP exhibited the shorter lifetime values (τ) and the lower intrinsic quantum yield (Φ_{Ln}). On the contrary, europium complexes **C1**, **C3** and **C5** based on the pentafluorinated β-diketone PFMP displayed much smaller nonradiative transition rates (A_{nrad}) in comparison with complexes **C2**, **C4** and **C6** and led to the decreasing radiative energy losses. Consequently, complexes **C1**, **C3** and **C5** exhibited the longer lifetime values (τ) and the higher intrinsic quantum yield (Φ_{Ln}). It is remarkable that from the present studies the lifetime values and intrinsic quantum yields obtained for europium complexes **C1** and **C3** were much higher than those of europium (III) complex with 4-methoxybenzoyltrifluoroacetone-Bipy ($\tau = 702$ μs; $\Phi_{\mathrm{Ln}} = 42.8\%$) or europium (III) complex with 4-methoxybenzoyltrifluoroacetone-Phen ($\tau = 741$ μs; $\Phi_{\mathrm{Ln}} = 48.1\%$) [44]. Especially, in these europium complexes, the complex **C1** with the ligands β-diketone PFMP and Bipy showed the longest lifetime value ($\tau = 814$ μs) and the highest intrinsic quantum yield ($\Phi_{\mathrm{Ln}} = 62.9\%$), which was probably attributed to the introduction of the auxiliary ligand Bipy with the higher flexibility and less steric hindrance resulting in the high affinity toward europium (III) ion [45]. It was in accord with the results from the excitation and emission intensity of the europium complex **C1**. Similarly, the complex **C2** with the ligands β-diketone PFAP and Bipy also revealed the longer lifetime value (τ) and the higher intrinsic quantum yield (Φ_{Ln}) compared with complexes **C4** and **C6** containing the auxiliary ligands Phen or Bath. It further indicated that the introduction of the auxiliary ligand Bipy was beneficial to the photoluminescence properties of these europium complexes, which was attributed to the higher flexibility of Bipy leading to better participation in the coordination of europium (III) ion.

Experimental intensity parameters

The Ω_t ($t = 2, 4$) intensity parameters can be obtained from experimental spectra, which is strongly dependent on the nature of the chemical environment around the europium (III) ion. To get insight into the possible information on the chemical environment of the emitting center europium (III) ion in these complexes, the experimental intensity parameters Ω_2 and Ω_4 were determined from the emission spectra of the europium (III) ion by the $^5\mathrm{D}_0 \rightarrow {}^7\mathrm{F}_2$ and $^5\mathrm{D}_0 \rightarrow {}^7\mathrm{F}_4$ transitions. Their values can be calculated from the equation [46]:

$$\Omega_t = \frac{3\hbar c^3 A_{0J}}{4e^2\omega^3\chi\left\langle {}^5D_0 \middle\| U^{(t)} \middle\| {}^7F_J \right\rangle^2}, \tag{4}$$

where A_{0J} (where $J = 2$ and 4) is the coefficient of spontaneous emission for the $^5\mathrm{D}_0 \rightarrow {}^7\mathrm{F}_J$ transition, Ω is the angular frequency of the transition, χ ($n_0^2(n_0^2+2)^2/9$, $n_0 = 1.5$) is the Lorentz local field correction and n_0 is the refractive index of the medium, $\langle {}^5D_0 \| U^{(2)} \| {}^7F_2 \rangle^2$ and $\langle {}^5D_0 \| U^{(4)} \| {}^7F_4 \rangle^2$ values are the squared matrix elements whose values are 0.0032 and 0.0023, respectively.

The obtained values of Ω_2 and Ω_4 for europium complexes **C1**–**C6** are shown in Table 2. It was pointed out that all europium (III) complexes exhibited the relatively high Ω_2 parameter values, which was interpreted as the hypersensitive behavior of the $^5\mathrm{D}_0 \rightarrow {}^7\mathrm{F}_2$ transition and indicated a highly polarizable chemical environment in these complexes. Compared with the β-diketone PFMP ligand, complexes **C2**, **C4** and **C6** with the β-diketone PFAP ligand displayed higher Ω_4 parameter values. This was probably because the steric PFAP ligands could prevent the auxiliary ligands from getting closer to the europium (III) ion and resulted in increasing the Ω_4 intensity parameter values [47].

Intramolecular energy transfer processes

To elucidate the energy transfer processes in these complexes, the singlet and triplet energy levels of ligands PFMP and PFAP were estimated by fitting a tangent at the higher wavelength edges of their UV–Vis absorbance and the lower wavelength emission edges of phosphorescence spectra for Gd^{3+} complexes [24]. Based on the UV–Vis absorption spectra (Fig. 2), the singlet energy levels (S_1) of ligands PFMP and PFAP were 27251 (367 nm) and 25843 (387 nm) cm^{-1}, respectively. According to the phosphorescence spectra for $Gd(PFMP)_3 \cdot 2H_2O$ and $Gd(PFAP)_3 \cdot 2H_2O$ (Fig. S1), the triplet energy levels of ligands PFMP and PFAP were 21370 (468 nm) and 21885 (457 nm) cm^{-1}, respectively. The singlet and triplet energy levels of auxiliary ligands bpy, phen and Bath were cited from the literature [24]. Their excitation energy parameters are presented in Table 3. Thus, the energy transfer processes were constructed and illustrated in Fig. 8 (complex **C1**) and Figs. S2–S6 (complexes **C2**–**C6**). Their energy transfer processes involved with the transfer of energy from the singlet state (S_1) to triplet state (T_1) of ligands and from T_1 state of ligands to the excited energy state of Eu(III) ion ($^5D_1$, 19,000 cm^{-1}, and $^5D_0$, 17,500 cm^{-1}).

From Table 3, the energy gap ΔE (T_1–Eu^{3+}) values between triplet states of these ligands to the resonating level of the europium ion were found in the range of 2000–5000 cm^{-1} as defined by Latva's empirical rule [48], which exhibited the efficient ligand-to-metal energy transfer process in complexes **C1**–**C6**. According to Reinhoudt's empirical rule [49], the intersystem crossing (ISC) process would be effective when ΔE (S_1–T_1) is at least 5000 cm^{-1}. The energy gap ΔE (S_1–T_1) values for PFMP, Phen, Bipy and Bath in ISC process were 5881, 7000, 8900 and 8000 cm^{-1}, respectively, which displayed the efficient ISC process in complexes **C1**, **C3** and **C5** with the ligand PFMP. However, the energy gap ΔE (S_1–T_1) value of ligand PFAP was 3958 cm^{-1} (<5000 cm^{-1}), which indicated that little effectiveness of the ISC process took place from the S_1 to T_1 in complexes **C2**, **C4** and **C6** with the ligand PAMP. Accordingly, the photoluminescence properties of complexes **C2**, **C4** and **C6** with the ligand PAMP were much weaker than those of complexes **C1**,

Table 3 The excitation energy parameters of ligands

Ligands	Singlet level (S_1)/cm^{-1}	Triplet level (T_1)/cm^{-1}	ΔE (S_1–T_1)/cm^{-1}	ΔE (T_1–Eu^{3+})/cm^{-1}
PFMP	27,251	21,370	5881	3870
PFAP	25,843	21,885	3958	4385
Bipy	29,900	22,900	7000	5400
Phen	31,000	22,100	8900	4600
Bath	29,000	21,000	8000	3500

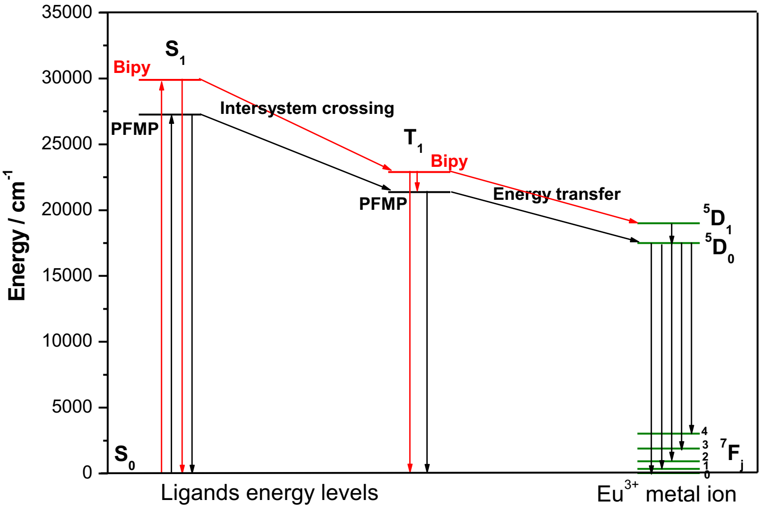

Fig. 8 The proposed energy transfer mechanism in Eu(PFMP)$_3$·Bipy (**C1**)

C3 and **C5** with the ligand PFMP. In addition, the lower energy gap *ΔE* (T$_1$–Eu^{3+}) value of ancillary ligand Bath could promote the inverse energy transfer and lead to the decrease in photoluminescence properties of europium (III) complexes with ligand Bath. This result was in agreement with the literature [50].

Thermogravimetric analysis

The thermal stability of europium complexes is essential for the luminescent materials, so thermal behaviors of complexes **C1**–**C6** were investigated by thermogravimetric analysis (TGA). The TG curves of these complexes are presented in Fig. 9. From these TG curves, complexes **C1**, **C3** and **C5** with the β-diketone PFMP ligand (Fig. 8a) exhibited the similar patterns of thermal decomposition as well as complexes **C2**, **C4** and **C6** with the β-diketone **PFAP** ligand (Fig. 8b).

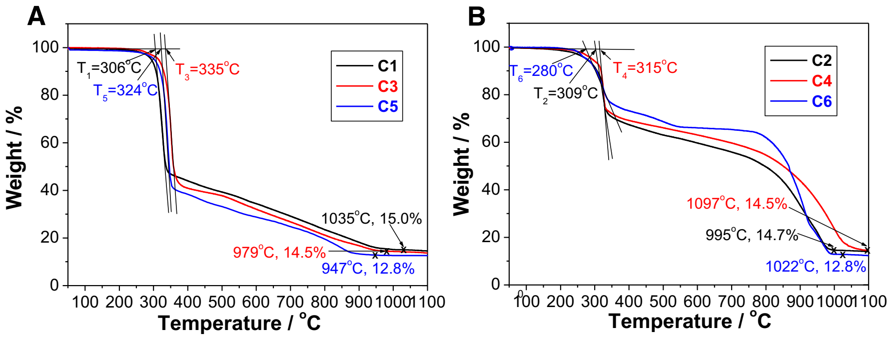

Fig. 9 TGA curves for complexes **C1**, **C3** and **C5** (**a**) and complexes **C2**, **C4** and **C6** (**b**)

These europium complexes involved two main successive mass loss steps from 50 to 1100 °C with the weight loss 85.0–87.2% due to elimination of the β-diketone or auxiliary ligand molecules. The final decomposition temperatures of complexes **C1**–**C6** were about 1035 °C, 995 °C, 979 °C, 1097 °C, 947 °C and 1022 °C, respectively, and their final residue of the decomposition was probably Eu_2O_3 because the final residue mass percentages of complexes **C1**–**C6** were 15.0%, 14.7%, 14.5%, 14.5%, 12.8% and 12.8%, respectively, which were in good agreement with the calculated values via their formula. In addition, the extrapolated initial decomposition temperatures of complexes **C1**–**C6** were about 306 °C, 309 °C, 335 °C, 315 °C, 324 °C and 280 °C, respectively, which were obtained according to their TG curves. The results of TGA curves indicate that these europium complexes synthesized have good thermal stability; they can be possibly used to fabricate some new optoelectronic devices.

Conclusions

In this work, six novel europium (III) complexes based on the pentafluorinated β-diketone, $Eu(PFMP)_3$·Bipy, $Eu(PFAP)_3$·Bipy, $Eu(PFMP)_3$·Phen, $Eu(PFAP)_3$·Phen, $Eu(PFMP)_3$·Bath and $Eu(PFAP)_3$·Bath, were designed, synthesized and characterized. The photophysical properties of these complexes were investigated in detail by UV–Vis and photoluminescence spectroscopy. The luminescence spectra for all complexes exhibited characteristic emission lines for europium ion in solid state and chloroform solution, which was due to transitions between the excited state ($^5D_0$) and the multiplet ($^7F_{0–4}$). Their luminescent decay curves and emission spectra indicated the presence of a single chemical environment around the emitting europium (III) ion in these complexes. The experiment intensity parameters, Ω_2 and Ω_4 were calculated from their emission spectra in solid state. The high Ω_2 values of these complexes suggested that the europium ion was located in a polarized chemical environment. Meanwhile, Europium (III) complexes **C1**, **C3** and **C5** with the β-diketone PFMP ligand displayed much better photoluminescence properties in comparison with complexes **C2**, **C4** and **C6** with the β-diketone PFAP ligand. The CIE chromaticity coordinates of complexes **C1**, **C3** and **C5** also presented high red color purity 100% ($x=0.67$, $y=0.33$). In particular, complex **C1** with β-diketone PFMP and Bipy ligands exhibited the longest lifetime value ($\tau=814$ μs) and the highest quantum yield ($\Phi_{Ln}=62.9\%$ and $\Phi=37.5\%$) in these complexes. The energy transfer process indicated the significance of the ligand as a good chromophore for the efficient energy transfer to the europium (III) ion. Additionally, TGA results showed that all complexes had excellent thermal stability, which were much more suitable for applications in optoelectronic devices.

Acknowledgements The authors gratefully acknowledge financial support from National Natural Science Foundation of China (No. 21542009) and Foundation for Hubei Key Laboratory of Pollutant Analysis and Reuse Technology (No. PA160203).

References

1. M.L. Di Lorenzo, M. Cocca, G. Gentile, M. Avella, D. Gutierrez, M.D. Pirriera, M. Kennedy, H. Ahmed, J. Doran, J. Colloid Interface Sci. **398**, 95 (2013)
2. P. Shukla, V. Sudarsan, R.K. Vatsa, S.K. Nayak, S. Chattopadhyay, J. Lumin. **130**, 1952 (2010)
3. F.-B. Wu, C. Zhang, Anal. Biochem. **311**, 57 (2002)
4. M.H.V. Werts, R.T.F. Jukes, J.W. Verhoeven, Phys. Chem. Chem. Phys. **4**, 1542 (2002)
5. G.F. De Sá, O.L. Malta, C. de Mello Donegá, A.M. Simas, R.L. Longo, P.A. Santa-Cruz, E.F. Da Silva Jr., Coord. Chem. Rev. **196**, 165 (2000)
6. H. Iwanaga, J. Lumin. **200**, 233 (2018)
7. Y.H. Pham, V.A. Trush, V.M. Amirkhanov, P. Gawryszewska, Opt. Mater. **74**, 197 (2017)
8. J.P. Martins, P. Martín-Ramos, C. Coya, M.R. Silva, M.E.S. Eusebio, A. de Andrés, Á.L. Álvarez, J. Martín-Gil, J. Lumin. **159**, 17 (2015)
9. C. Yang, J. Xu, J. Ma, D. Zhu, Y. Zhang, L. Liang, M. Lu, Polym. Chem. **3**, 2640 (2012)
10. Y. Wang, H. Wang, X. Zhao, Y. Jin, H. Xiong, J. Yuan, J. Wu, New J. Chem. **41**, 5981 (2017)
11. K. Kuriki, Y. Koike, Y. Okamoto, Chem. Rev. **102**, 2347 (2002)
12. B. Rajamouli, S. Kasturi, S. Giri, V. Sivakumar, Inorg. Chem. **56**, 10127 (2017)
13. B. Rajamouli, C.S.D. Viswanath, S. Giri, C.K. Jayasankar, V. Sivakumar, New J. Chem. **41**, 3112 (2017)
14. D.B. Ambili Raj, S. Biju, M.L.P. Reddy, Dalton Trans. **36**, 7519 (2009)
15. R. Devi, M. Bala, S.P. Khatkar, V.B. Taxak, P. Boora, J. Fluor. Chem. **181**, 36 (2016)
16. X. Zhao, Z. Hou, B. Wang, Q. Shen, H. Jia, A. Zhang, X. Liu, B. Xu, Res. Chem. Intermed. **43**, 4129 (2017)
17. B. Rajamouli, P. Sood, S. Giri, V. Krishnan, V. Sivakumar, Eur. J. Inorg. Chem. **24**, 3900 (2016)
18. S. Kasturi, B. Rajamouli, V. Sivakumar, Inorg. Chem. **56**, 9376 (2017)
19. B. Rajamouli, V. Sivakumar, ChemistrySelect **2**, 4138 (2017)
20. B. Rajamouli, V. Sivakumar, J. Photochem. Photoboil. A **347**, 26 (2017)
21. D. Wang, Y. Pi, H. Liu, X. Wei, Y. Hu, J. Zheng, J. Alloys Compd. **613**, 13 (2014)
22. D. Wang, H. Liu, L. Fan, G. Yin, Y. Hu, J. Zheng, Synth. Met. **209**, 267 (2015)
23. D. Wang, C. Zheng, L. Fan, Y. Hu, J. Zheng, Spectrochim. Acta Part A **117**, 245 (2014)
24. D.B. Ambili Raj, S. Biju, M.L.P. Reddy, Inorg. Chem. **47**, 8091 (2008)
25. B. Francis, D.B. Ambili Raj, M.L.P. Reddy, Dalton Trans. **39**, 8084 (2010)
26. D.B. Ambili Raj, B. Francis, M.L.P. Reddy, R.R. Butorac, V.M. Lynch, A.H. Cowley, Inorg. Chem. **49**, 9055 (2010)
27. V. Divya, M.L.P. Reddy, J. Mater. Chem. C **1**, 160 (2013)
28. J.N. Demas, G.A. Crosby, J. Phys. Chem. **75**, 991 (1971)
29. C. Yang, J. Luo, J. Ma, M. Lu, L. Liang, B. Tong, Dyes Pigments **92**, 696 (2011)
30. L.R. Melby, N.J. Rose, E. Abramson, J.C. Caris, J. Am. Chem. Soc. **86**, 5117 (1964)
31. Y. Zhang, H. Shi, Y. Ke, Y. Cao, J. Lumin. **124**, 51 (2007)
32. L. Fu, R.A.S. Ferreira, N.J.O. Silva, A.J. Fernandes, P. Ribeiro-Claro, I.S. Goncalves, V. de Zea Bermudez, L.D. Carlos, J. Mater. Chem. **15**, 3117 (2005)
33. N.S. Bhacca, J. Selbin, J.D. Wander, J. Am. Chem. Soc. **94**, 8719 (1972)
34. K. Iftikhar, Polyhedron **15**, 1113 (1996)
35. V. Sareen, R. Gupta, J. Fluor. Chem. **76**, 149 (1996)
36. X. Jiang, Y. Wu, C. He, Mater. Lett. **62**, 286 (2008)
37. K. Nakamoto, *Infrared and Raman Spectra of Inoganic and Coordination Compounds*, 6th edn. (Wiley, New Jersey, 2009), p. 23
38. M.C.F.C. Felinto, C.S. Tomiyama, H.F. Brito, E.E.S. Teotonio, O.L. Malta, J. Solid State Chem. **171**, 189 (2003)
39. O.L. Malta, H.F. Brito, J.F.S. Menezes, F.R.G. e Silva, S. Alves Jr., F.S. Farias Jr., A.V.M. de Andrade, J. Lumin. **75**, 255 (1997)
40. P. He, H. Wang, S. Liu, W. Hu, J. Shi, G. Wang, M. Gong, J. Electrochem. Soc. **156**, E46 (2009)
41. A. Beeby, I.M. Clarkson, R.S. Dickins, S. Faulkner, D. Parker, L. Royle, A.S. de Sousa, J.A.G. Williams, S.M. Wood, J. Chem. Soc. Perkin Trans. **2**, 493 (1999)
42. J.R. Lakowicz, *Principles of Fluorescence Spectroscopy*, 3rd edn. (Springer, New York, 2006), p. 99

43. R. Ferreira, P. Pires, B. de Castro, R.A.S. Ferreira, L.D. Carlos, U. Pischel, New J. Chem. **28**, 1506 (2004)
44. D. Wang, Z. Luo, Z. Liu, D. Wang, L. Fan, G. Yin, Dyes Pigments **132**, 398 (2016)
45. R. Devi, Priyanka, S. Chahar, S.P. Khatkar, V.B. Taxak, P. Boora, Inorg. Chim. Acta **471**, 364 (2018)
46. M.O. Rodrigues, N.B. da Costa Júnior, C.A. de Simone, A.A.S. Araújo, A.M. Brito-Silva, F.A. Almeida Paz, M.E. de Mesquita, S.A. Júnior, R.O. Freire, J. Phys. Chem. B **112**, 4204 (2008)
47. A.A.S. Araújo, H.F. Brito, O.L. Malta, J.R. Matos, E.E.S. Teotonio, S. Storpirtis, C.M.S. Izumi, J. Inorg. Biochem. **88**, 87 (2002)
48. M. Latva, H. Takalo, V.M. Mukkala, C. Matachescu, J.C. Rodriguez-Ubis, J. Kankare, J. Lumin. **75**, 149 (1997)
49. F.J. Steemers, W. Verboom, D.N. Reinhoudt, E.B. van der Tol, J.W. Verhoeven, J. Am. Chem. Soc. **117**, 9408 (1995)
50. R. Devi, M. Dalal, M. Bala, S.P. Khatkar, V.B. Taxak, P. Boora, J. Mater. Sci. Mater. Electron. **27**, 12506 (2016)